

Modeling of Selforganizing Systems

Cordula Rauwolf, and Thomas Straßner^{†,*}

Organische Chemie, TU Dresden, Mommsenstraße 13, D-01062 Dresden, Germany (strasner@organik.uni-erlangen.de)

[†] Present address: Dept. of Chemistry and Biochemistry, UCLA, Los Angeles, California 90095-1569, USA

Received: 23 September 1996 / Accepted: 3 December 1996 / Published: 17 January 1997

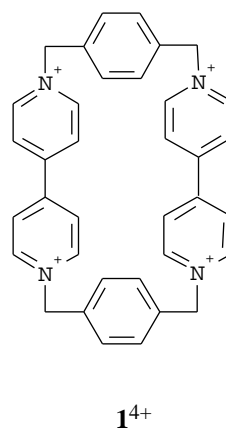
Abstract

The concept of self-assembly developed for the construction of topologically complex molecules such as [2]-catenanes and rotaxanes is based on non-covalent interactions between constituent parts. High product yields are explained by favourable orientations of intermediates. These intermediates are found to be 2 - 9 kcal/mol lower in energy than the reactand ground states and the recognition process could be reproduced by semiempirical calculations using the PM3 Hamiltonian. Cyclobis(paraquat-p-phenylene) ($\mathbf{1}^{4+}$), which is known for its extraordinary capability to form charge-transfer complexes, plays an important role. The conformational analysis of the hypersurface of ($\mathbf{1}^{4+}$) and other compounds was performed using the MM2 force field. The concept of self-organization uses electron accepting hosts like $\mathbf{1}^{4+}$ as well as donating hosts like crown ethers. Therefore the study was extended on donating hosts and on their capability to form catenanes. These very interesting compounds show stabilization energies of about 36 kcal/mol.

Keywords: Self-organization, semiempirical calculation, catenanes, complexation, supramolecular chemistry

Introduction

The concept of self-organization [1] was introduced some years ago. J.F. Stoddart, a pioneer of the concept, described the formation of several complex macrocyclic structures. Especially Cyclobis(paraquat-p-phenylene) ($\mathbf{1}^{4+}$), the synthesis published in 1988 [2], has been used to prepare a variety of self-assembled rotaxanes and catenanes [3]. An extraordinary example for the success of the strategy was the synthesis of 'Olympiadan' in 1994 [4]. Compound $\mathbf{1}^{4+}$ forms inclusion complexes with a variety of compounds including amino acids [5], benzene derivatives [6] and π -donors like tetrathiafulvalene [7]. The template synthesis concept was used with great success by several groups to create



Scheme 1. Cyclobis(paraquat-p-phenylene)

* To whom correspondence should be addressed

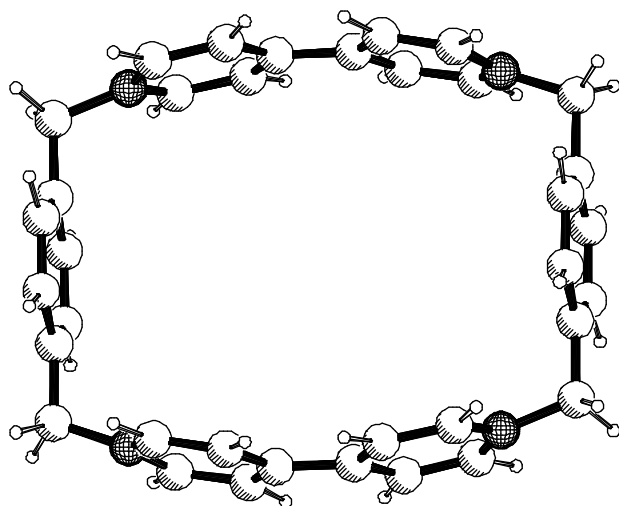
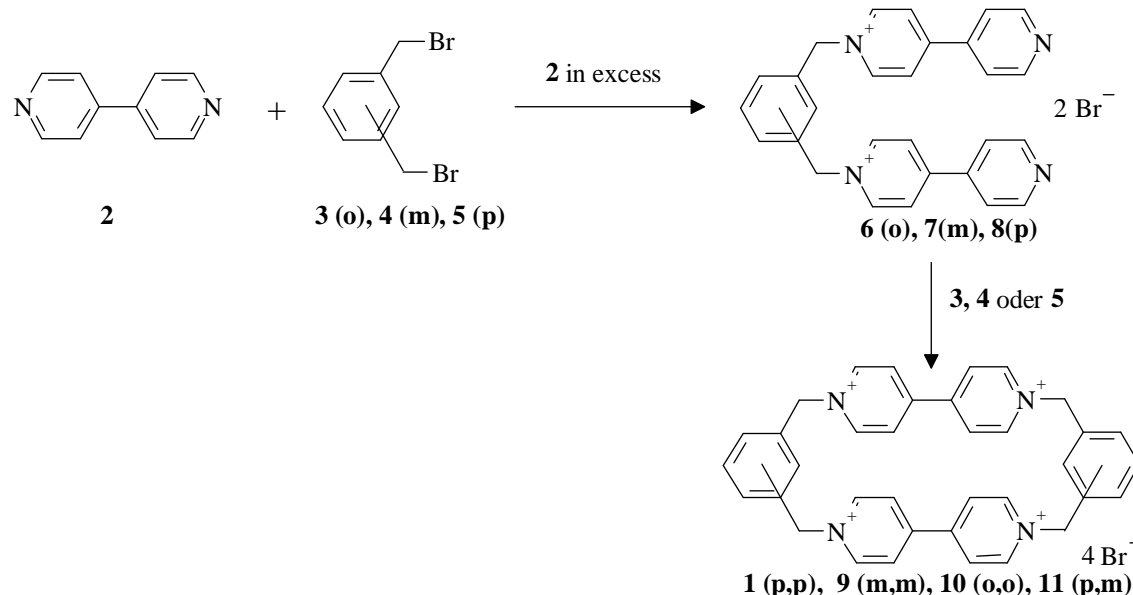
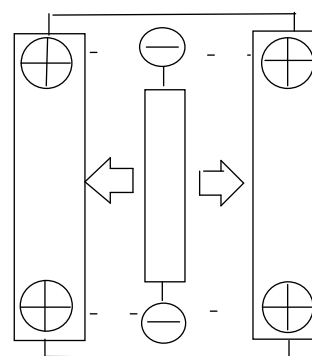


Figure 1. Cyclobis(paraquat-p-phenylene), optimized with the PM3 Hamiltonian (I^{4+})

macrocycles and catenans with different capabilities [8]. Self-organization means that the interaction between two molecules leads to a complex structure, which is lower in energy than that of the separate molecules and shows a favourable geometrical position for ring closure and high product yields. The energy contribution comes from effects like donor-acceptor-interaction, π -stacking and hydrogen bonds [9]. These small forces are difficult to describe with theoretical models and an ab initio approach would be highly desirable. But due to the size of those systems ab initio calculations are not

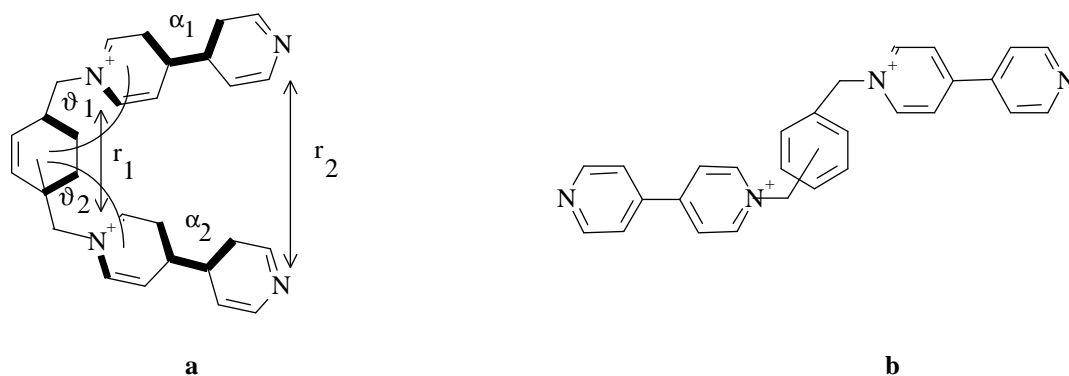


Scheme 3. Synthesis of cyclophanes I^{4+} (p,p), 9 (m,m), 10 (o,o), 11 (p,m) [17].



Scheme 2. Donor-acceptor interaction of a tetracationic host with a donor-compound

feasible at least for a series of compounds. Force field calculations do not consider electronic effects and are therefore useless for this problem, because electronic effects play an important role. The influence of counterions as well as solvent effects on the electrostatics have been studied. This study is intended to show that the formation of those complex self-organized structures can be calculated with semiempirical methods, which are known to be able to calculate hydrogen bonds and π - π interactions [10].



Scheme 4. Size of the cavity of *a*- isomer dications and scheme of *b*- isomer dications.

Table1. Description of the cavity of different *a*-isomer dications.

	PM3			AM1			MNDO		
	6a	7a	8a	6a	7a	8a	6a	7a	8a
Link	2	4	6		9	11		13	15
r_1	5.45	6.98	7.25	—*	7.21	7.32	—*	7.19	7.47
r_2	17.30	16.89	14.80		18.32	15.72		17.65	16.42
α_1	359.81	359.85	359.95		32.44	32.41		279.04	261.36
α_2	359.83	0.13	0.02		327.55	327.27		262.67	80.77
θ_1	294.15	39.19	358.66		308.69	326.73		199.14	327.69
θ_2	20.64	350.34	0.98		51.19	23.14		161.16	326.40

* not converged

Computational procedure

We used the PM3-Hamiltonian [11] in form of the computing package VAMP 5.0 [12] (running on a CONVEX C220 and an IBM-590) together with the EF-optimizer [13]. Unless otherwise noted, all structures were calculated using the keyword PRECISE. The conformational hypersurface was searched by the MLTOR-option in PCMODEL 3.0 [14], all resulting structures minimized by the MM2 force field [15]. The force field minimization was followed by a full optimization without constraints using PM3. The electrostatic maps were generated by Spartan 4.0 [16]. All geometries are provided as threedimensional pictures (xyz-coordinates), the supplementary material is available on request.

Interaction of Cyclobis(paraquat-p-phenylene) with various guest molecules

Cyclobis(paraquat-p-phenylene) 1^{4+} is a tetracation which shows extraordinary capability to form inclusion charge transfer complexes with donor molecules (see scheme 2). The synthesis itself is a self-organized process, where two molecules of 4,4'-bipyridine **2** react under phase transfer conditions with *o*-xylene **3**, *m*-xylene **4** or *p*-xylene **5** to form the corresponding dications **6** – **8**, which are preorganized for the ring-closure with another xylene molecule [17], as shown in scheme 3. X-ray data of 1^{4+} [18] and **9** [19] are useful to compare the computational results.

The dications can form two isomers. As long as both bipyridyl units are on the same side we call them *a*-isomers, if they are on opposite sides they are called *b*-isomers. The size of the cavity seems to play an important role for the interaction between the host and the guest molecule. The cavity of the *a*-isomer dications is measured as described in

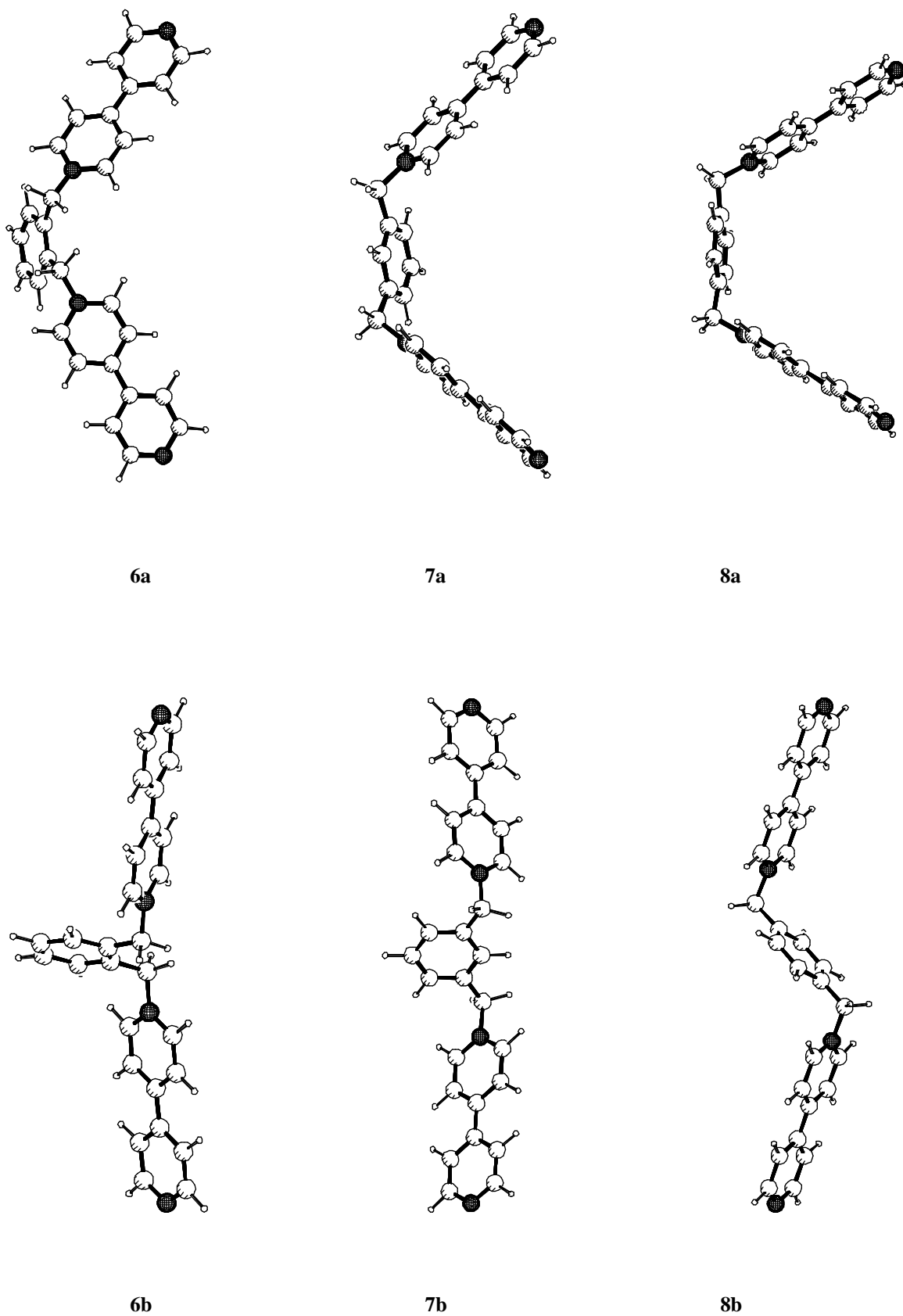


Figure 2. Comparison of PM3 optimized structures 6a to 8b

Table 2. Heat of formation of different dications

Heat of formation in kcal/mol						
	PM3	Link	AM1	Link	MNDO	Link
6a	507.90	2	—*		—*	
6b	505.40	3	523.80	8	—*	
7a	498.79	4	515.62	9	516.43	13
7b	497.44	5	514.70	10	514.85	14
8a	497.37	6	514.91	11	515.22	15
8b	495.59	7	513.51	12	513.61	16

* not converged

scheme 4. The distances r_1 and r_2 are measured between the nitrogen atoms, the angles α_1 and α_2 give the torsion within the bipyridine unit, ϑ_1 and ϑ_2 are the torsional angles between the planes of the bipyridine and phenylene rings. Table 1 gives the size of the cavity of all **a**-isomer dications, while table 2 compares the heat of formation of all possible dications.

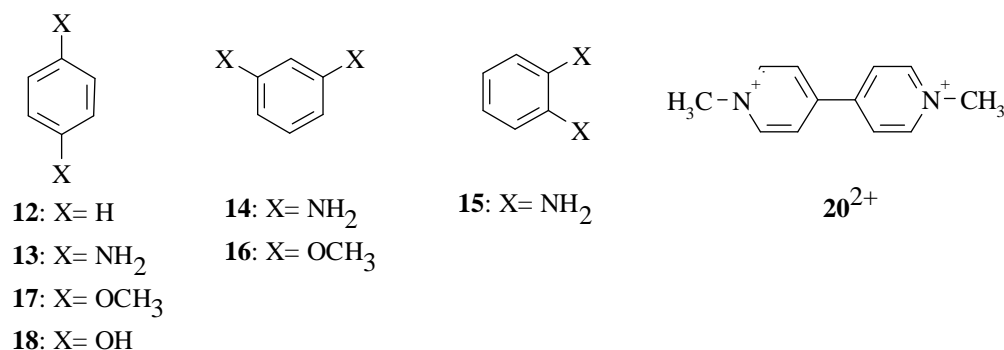
The most obvious difference is the geometry of the bipyridine unit (cf. figure 2). It is similar over all three isomers and depends only on the Hamiltonian used. PM3 calculates this unit as almost planar, while AM1 gives an dihedral angle in the bipyridine unit α_1 of about 30° . MNDO is even

more extreme and calculates a value of about 90° for α_1 and α_2 , i.e. no conjugation within the bipyridyl unit. These results for α_1 and α_2 influence the distances r_1 and r_2 . The r_1 distances are more or less fixed and indifferent, but the r_2 distances differ a lot. The distances show that the 'scissors' open up wide to avoid strain contributions to their energy. PM3 calculates the shortest distances, which means that the structure is most preorganized for cyclization.

The torsional angles ϑ_1 and ϑ_2 give insight into the conformation of the macrocycle, into the twist between the aromatic ring and the plane of the bipyridyl unit. In the case of the para-substituted benzene all methods calculate the smallest twist angle. With PM3 the structure is almost not twisted, with MNDO and AM1 to a low degree of about 33° and 23° , respectively. The large differences in the twist angles of structure **7a** (PM3: 39.2° , MNDO: 161.9° , AM1: 51.3°) show the

Table 3. Interaction energy between host **8a** and guests **12** and **13**

PM3		Host 8a		
Guest	Energy of guest ΔH_f (kcal/mol)	Host- Guest- Energy ΔH_f (kcal/mol)	Energy difference (kcal/mol)	Link
12	23.45	518.42	-2.42	17
13	19.66	511.21	-5.89	18

**Scheme 5.** Different compounds used as guest molecules

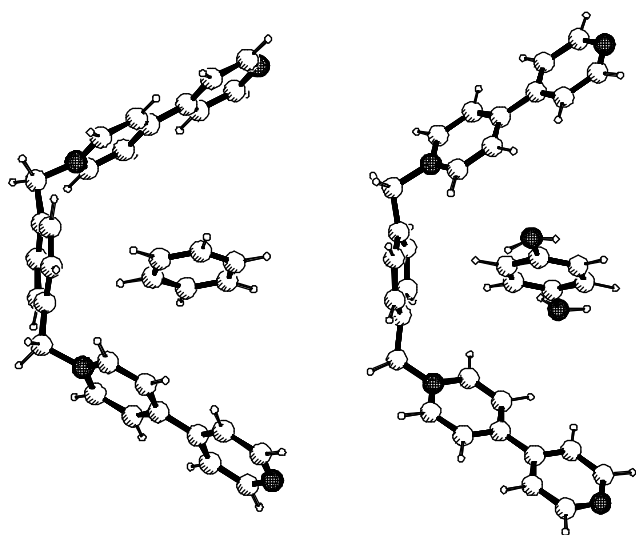


Figure 3. Host **8a** with intercalated guests **12** and **13**, according to a PM3 calculation

influence of the used Hamiltonian. Due to the twist angle we had to take into account both possible conformations (**9a**, **9b**) of macrocycle **9** (see scheme 6).

The first step of the self-organization process which leads to catenanes has to be the formation of a molecular system where a compound like **6**, **7** or **8** is favoured in the **a**-form (cf. figure 2). But independent of the Hamiltonian used, the **b**-isomers are more stable. The differences are small, according to PM3 the **b**-isomers are between 1.3 and 2.5 kcal/mol more stable than the corresponding **a**-isomers (table 2). The results of the MNDO calculations are in both cases (**7b** vs. **7a**, **8b** vs. **8a**) that the **b**-isomers are 1.6 kcal/mol more stable. AM1 calculates the lowest differences of about 0.9 to 1.4 kcal/mol.

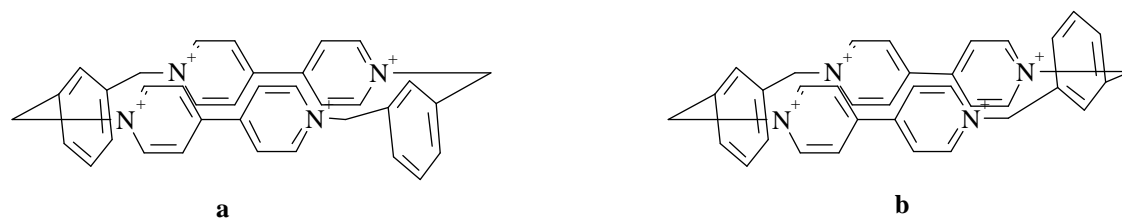
But as soon as an acceptor guest molecule (scheme 5), e.g. benzene (**12**) or p-phenylenediamine (**13**) is intercalated into the molecular tweezers of host **8a** (cf. figure 3) the systems is lower in energy compared to the sum of the energies of the single compounds. No interaction between **8b** and compounds **12** or **13** could be found.

The negative interaction energy between the aromatic rings of **8a** and **12** results from π - π interaction, while **13** can additionally act as a donor with its NH_2 -group. The complex **8a/12** shows no torsional angles ϑ_1 or ϑ_2 with the benzene molecule exactly in the middle of the tweezer. The aromatic units are stacked in a distance of 5.1 Å and the distance r_2 is reduced to 14.5 Å. Complex **8a/13** is different, ϑ_1 and ϑ_2 show a significant torsion of 28.97 and 28.86 degrees and the NH_2 -groups of guest molecule **13** interact with the aromatic rings. No interaction between the nitrogens of the bipyridyl unit and **13** could be found.

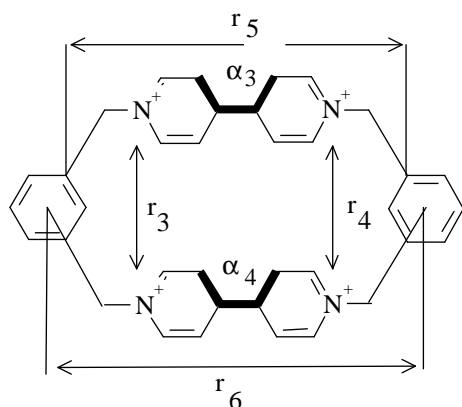
Conformational analysis of macrocycles (**1⁴⁺**) and (**9**)

A detailed search of the conformational hypersurface of compounds (**1⁴⁺**) and (**9**) was conducted. The PCModel 3.0 [14] option 'MLTOR' was used to generate starting geometries for further optimization. All $-\text{X}-\text{CH}_2-$ bonds were rotated in 30° degree increments. The search for compound (**1⁴⁺**) resulted in 33 different conformers, for compound (**9**) we received 58 conformers. For optimization only the PM3 Hamiltonian was used, because due to previously discussed results, MNDO and AM1 were not expected to provide more information. After the semiempirical optimization, only two conformers with different symmetry were received for (**1⁴⁺**). The D_{2h} -symmetrical compound ($\alpha_3, \alpha_4 = 0^\circ$) is calculated to be 0.9 kcal/mol more stable than the C_1 -symmetrical compound ($\alpha_3, \alpha_4 = 32.8^\circ$). The conformational analysis of compound (**9**) resulted in two different structures too. They depend on the above mentioned torsional angles ϑ_1 and ϑ_2 and therefore one shows 'chair-' and one 'boat' geometry (cf. scheme 6). All minimum structures were then optimized by MNDO and AM1 to compare the three semiempirical Hamiltonians. Also for compound **10** two different isomers have to be considered. The isomers, where all phenylene units point into one direction ('boat') are described as isomer **a**, those pointing in the other direction ('chair') as **b**. Scheme 6 gives a formula representation of compounds **9a** and **9b**.

Scheme 7 describes how the size of the cavity in all tetracationic cyclophanes was measured: r_3, r_4 give the distances between the nitrogen atoms and r_5, r_6 the distances between the hydrogen free carbon atoms of the o-, m- or p-



Scheme 6. Tetracationic isomers **9a** (boat) and **9b** (chair).



Scheme 7. Size of the cavity of tetracationic cyclophanes.

Table 4. Cavity of tetracationic cyclophanes and comparison of heat of formation in PM3 method

PM3	1 ⁴⁺	9a	9b	10a	10b	11
Link	1	19	20	21	22	23
r₃	6.86	5.93	5.95	4.14	4.13	6.08
r₄	6.86	5.93	5.95	4.14	4.13	6.76
r₅	9.75	10.21	10.28	10.57	10.77	9.93
r₆	9.75	10.21	10.28	10.57	10.77	9.93
α₃	0.00	322.43	358.95	0.00	357.83	36.34
α₄	0.00	322.41	1.05	0.00	2.20	323.37
ΔH_f (kcal/mol)	1070.90	1079.59	1078.17	1113.12	1113.13	1076.36

Table 5. Cavity of tetracationic cyclophanes and comparison of heat of formation in AM1 method

AM1	1 ⁴⁺	9a	9b	10a	10b	11
File	24	25	26	27	28	29
r₃	6.87	5.80	5.80	3.98	4.03	6.02
r₄	6.87	5.80	5.80	3.98	4.03	6.74
r₅	9.77	10.46	10.54	10.72	10.93	10.06
r₆	9.77	10.46	10.52	10.72	10.93	10.06
α₃	32.62	326.43	327.00	331.73	332.70	31.50
α₄	327.37	326.44	325.36	331.73	27.32	328.48
ΔH_f (kcal/mol)	1092.91	1096.62	1096.65	1129.81	1129.56	1095.87

phenylene bridge. Torsional angles α_3 and α_4 describe the torsion within the bipyridine unit.

Tables 4-6 compile geometrical parameters of all tetracationic cyclophanes together with their heat of formation values in dependence of the used Hamiltonian.

For compound 1⁴⁺ all Hamiltonians calculate the largest box of all macrocycles considered (cf. figure 4). The experimentally often used system 1⁴⁺ is also the compound of lowest energy. The size of the cavity of 11 is comparable, but 11 shows a strong torsion in the bipyridine unit ($\alpha_3, \alpha_4 = 36.5$ degree), which results in an unfavourable interaction with the guest molecule. The molecular complex of 11 with a guest molecule has to loose energy to planarize the bipyridyl unit before a favourable interaction with a guest molecule can take place.

Compounds 9a and 9b show only with PM3 an energy difference. PM3 favours the 'chair'-conformation, which was experimentally found with the X-ray structure [19], to be 7.3 kcal/mol higher in energy as 1⁴⁺. AM1 and MNDO calculate

Table 6. Cavity of tetracationic cyclophanes and comparison of heat of formation in MNDO method

MNDO	1⁴⁺	9a	9b	10a	10b	11
File	30	31	32	33	34	35
r_3	6.94	5.89	5.88	4.14	4.11	6.15
r_4	6.94	5.89	5.88	4.14	4.11	6.86
r_5	9.93	10.57	10.62	10.92	11.15	10.12
r_6	9.93	10.57	10.71	10.92	11.10	10.12
α_3	51.19	303.76	301.14	302.81	303.54	55.06
α_4	51.21	303.77	306.65	302.81	302.28	304.94
ΔH_f (kcal/mol)	1106.71	1111.65	1111.66	1154.55	1154.69	1108.93

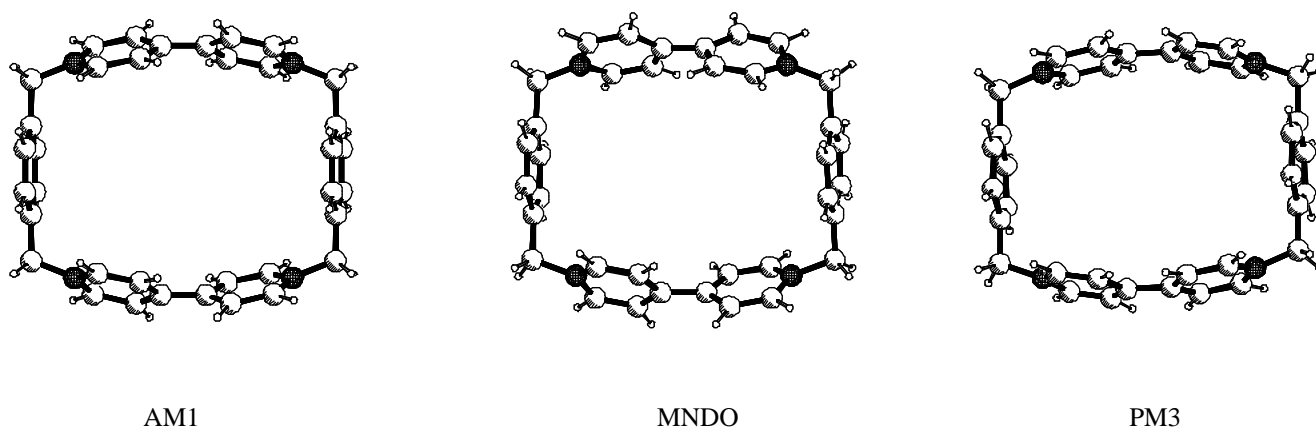
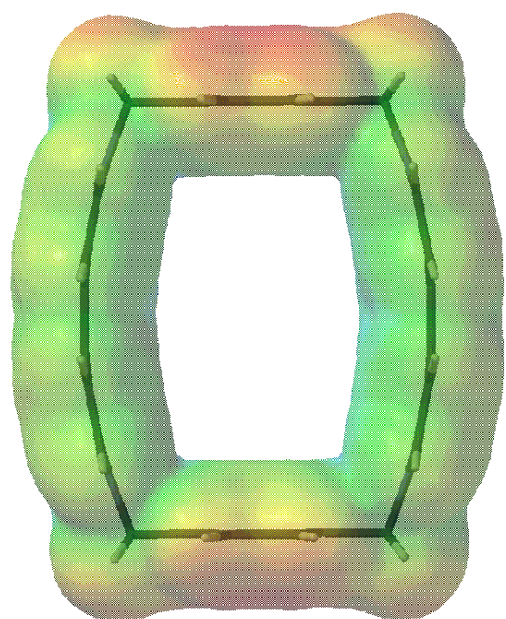


Figure 4. Compound **1⁴⁺** calculated with all three different Hamiltonians AM1, MNDO and PM3

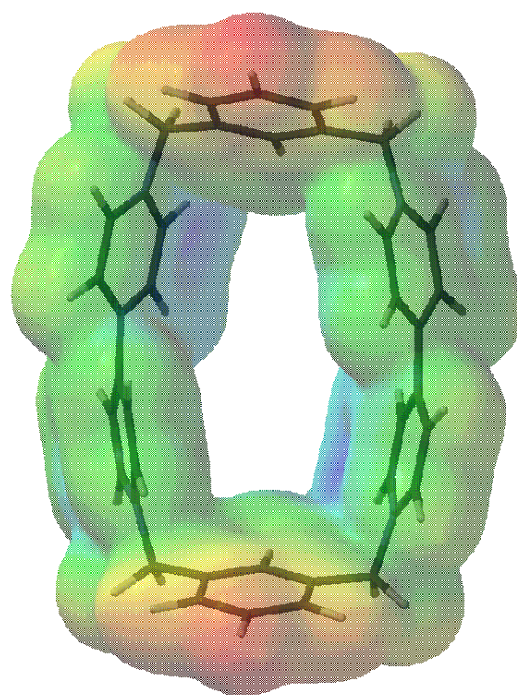
both isomers of even energy with a lower difference to **1⁴⁺** (AM1: 3.7 kcal/mol; MNDO: 4.9 kcal/mol). There is only a small energy difference between the **a** and **b**- isomers, however, the energy difference between the different hosts is significant. For compounds **10a** and **10b** all Hamiltonians calculate both isomers to have similar energy and to be at least 34 kcal/mol (PM3) higher in energy than compound **9**! The shape of **10** is a very narrow box, what is obvious in figure 5, where the electrostatic surfaces of compounds **1⁴⁺**, **9**, **10** and **11** are compared. The three Hamiltonians calculate almost identical numerical values for the distances r_3 to r_6 , while again the bipyridyl unit is treated different. The results for the torsional angles α_3 and α_4 are similar to those discussed before for the systems **6a** to **8a**. Except in the cases of **9a** and **11** PM3 again calculates the bipyridyl unit to be planar, while AM1 (about 30 degree) and MNDO (about 55 degree) show

considerable twisting. Compared to the experimental X-ray structures [18,19] PM3 again proved to be the most useful Hamiltonian.

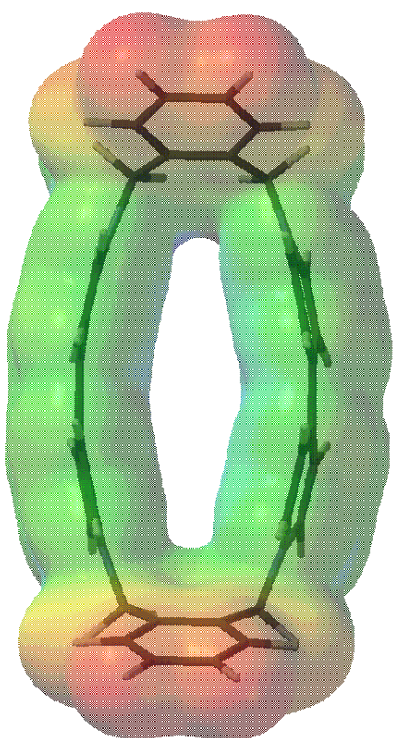
The electrostatic map could provide further insight into the nature of the interaction. Therefore we created the electrostatic map of compounds **1⁴⁺**, **9**, **10** and **11**. They are shown in figure 5. The molecular electrostatic potential of all four compounds is mapped onto the electron density surface. Red indicates regions with the most negative electrostatic potential and blue indicates regions with the most positive electrostatic potential. In general the most negative part is the outside of the phenyl ring depending on the geometry of the molecule and the most positive part is inside of the cavity towards the nitrogen atoms. But the extent and the potential are different. Compound **11** combines the steric effect of m- and p-substitution. The para-substitution leads to a better distribution of the electron density. This is encoded by the lower intensity of the colours shown, while at the meta end the red colour is especially notable in the upper part of the phenyl ring. The inside of **11** is sharing the positive electron density,



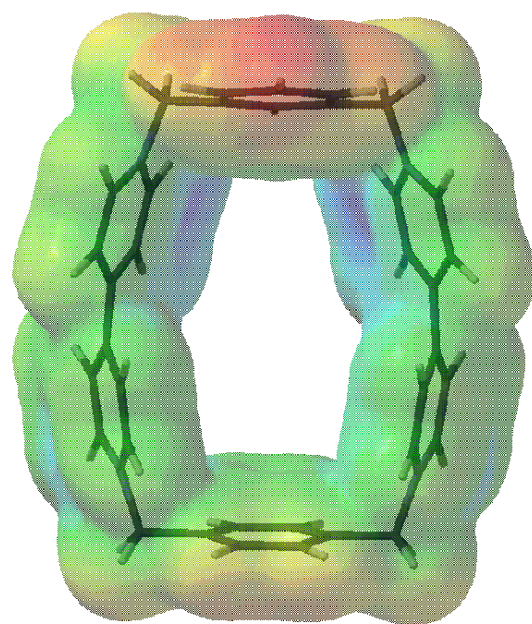
1



9



10



11

Figure 5. Electrostatic maps of sterically different macrocycles 1^{4+} , 9, 10 and 11

Table 7. ΔH_f of single guest compounds (donor) as well as H_f of the complexes of macrocycle 1^{4+} with different guests and their interaction energy

PM3	Host 1^{4+}			
Guest	Energy of guest ΔH_f (kcal/mol)	Energy of complex $1^{4+} + \text{Guest}$ ΔH_f (kcal/mol)	Interaction energy (kcal/mol)	Link
12	23.45	1092.10	-2.25	36
13	19.66	1083.54	-7.02	37
14	19.17	– *	– *	–
15	22.21	1081.70 **	-11.41	38
16	-52.61	1003.55 **	-14.74	39
17	-51.89	1010.12	-8.89	40
18	-65.98	1004.61	-0.31	41
18**	-65.98	998.09 **	-6.83	42

* no inclusion complex could be found

** not exactly incorporated, slight displacement

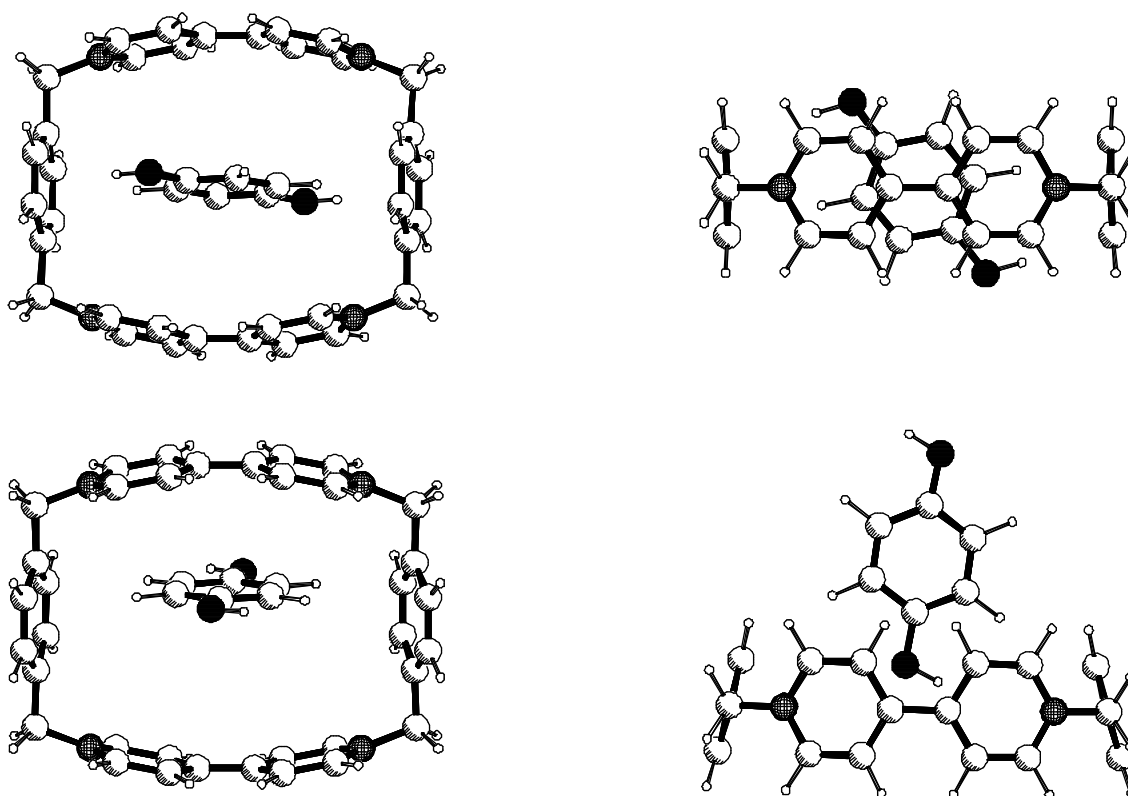


Figure 6. Compounds 18 and 18** in top and side view explain the displacement of the guest molecule.

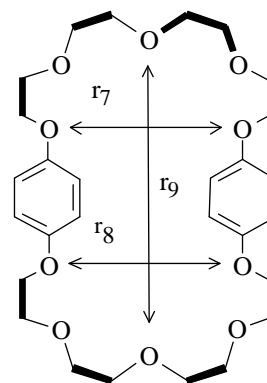
while the colour coding of the nitrogens at the meta end is more intense than at the opposite side. This effect is also notable at compound **10**. The geometry of **10** leads to a red coding on the outside of the upper part of the phenyl ring and a blue coding inside the macrocycle with a deep blue region around the nitrogen atoms. Compound **9** and even more compound **1⁴⁺** show a different electron density distribution, so the intensity of the colour coding is lower. The electron density distribution of **1⁴⁺** is the smallest of these four compounds, which might result from the lower steric repulsion.

But the host-guest interaction does not only depend on the electron density. To incorporate donor compounds the host needs a cavity which is also large enough to have not too much unfavourable contacts. To our knowledge there has never been a publication about inclusion complexes of **9** and **10**, which can be understood from figure 5. The distance between the electrostatic surfaces leaves not enough space for a guest compound, while **11** should be able to incorporate guests.

Typical donor molecules are shown in scheme 5: benzene (**12**), p-phenylenediamine (**13**), m-phenylenediamine (**14**), o-phenylenediamine (**15**), m-dimethoxybenzene (**16**), p-dimethoxybenzene (**17**) and p-dihydroxybenzene (**18**).

Complexes with compound **1⁴⁺** could be found for almost every donor molecule (see table 7), while the cavity of compounds **9**, **10** and also **11** proved to be too small to give stable host-guest-complexes. During the optimization the guest sometimes was displaced along the central axis due to unfavourable interaction energies. For compound **1⁴⁺** there are several molecular charge-transfer complexes known in literature [2,5b,6b,7]. It was possible to reproduce these experimentally known geometries. The host molecule **1⁴⁺** acts as an acceptor to several donors. The molecular complex between **1⁴⁺** and **17** is an example where the guest is displaced from the optimal arrangement for π -stacking due to a more favourable electrostatic interaction between one of the methoxy oxygens and the nitrogen atoms. The methoxy group is known as a moderate π -electron donating substituent [20] and additionally stabilizes the complex. The electrostatic surface of the complex **1⁴⁺/17** shows a red (negative) region where the other oxygen, which is not interacting with the nitrogen atoms, is pointing out of the complex. The interaction of the second methoxy group with the nitrogen atoms results in an electrostatic surface where no red coloring is visible. The partial charges on the nitrogen atoms close to the oxygen atoms of the methoxy group are influenced by the interaction and show a more positive partial charge, which is stabilized by the donation of the methoxy group. This results in the highest stabilization of all studied guests.

Figure 6 shows two molecular complexes between **1⁴⁺** and **18**. The displaced structure is 6.5 kcal/mol more stable than the structure where **18** is fully incorporated. The most probable explanation for the energy difference is the existence of repulsive forces between the phenyl rings in the complex **1⁴⁺/18**. Both are minima on the hypersurface.



19

Scheme 9. Bisparaphenylene-[34]crown-10.

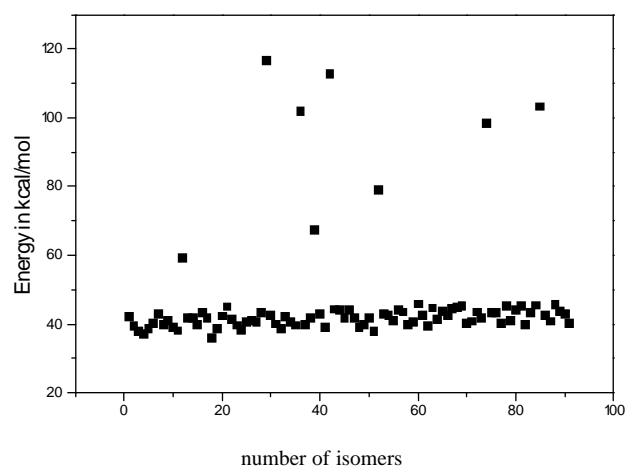


Figure 7. Steric energy distribution of all 91.

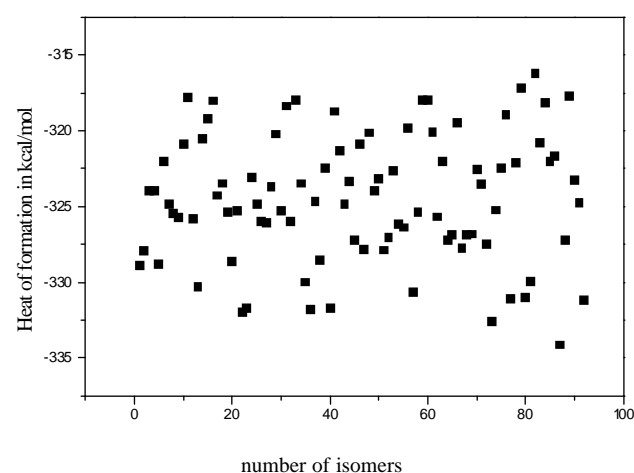
Figure 8. Energy distribution (ΔH_f) of all 91 conformers after MM2-optimization conformers after PM3-optimization.

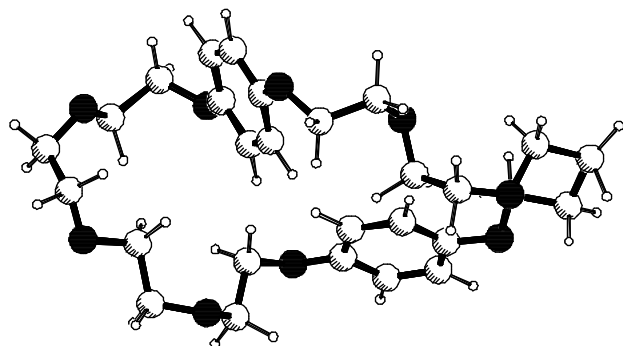
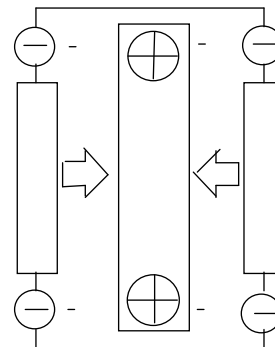
Table 9. Size of the cavity and heat of formation of **19**, calculated with PM3

PM3	19a	19b
Link	43	44
r_7	4.74	10.11
r_8	8.18	9.52
r_9	11.15	11.36
ΔH_f (kcal/mol)	-334.14	-316.26

The interaction energy between the electron accepting host 1^{4+} and donating guests is calculated to be between 2 and 9 kcal/mol. This is enough to stabilize structures which are preorganized for the formation of catenanes. The calculated intermediates provide insight into the mechanism of the self-organization process which is experimentally known for compound 1^{4+} , where the self-organization accounts for high product yields.

But it is known [21] that the self-organization process is also useful with donating host molecules and electron accepting guests, which are incorporated as sketched in scheme 8.

As a model system bisparaphenylene-[34]crown-10 (**19**) was used. A thorough conformational analysis was conducted to investigate the conformation of the host molecule. The same methodology described before for the analysis of 1^{4+} and **9** was used to conduct the conformational analysis. The structure is very flexible and possesses many degrees of freedom. A full approach would consider all the torsions over all bonds, but due to the multidimensionality of the problem

**Figure 9.** Comparison of structures **19a** and **19b**, optimized with PM3.**Scheme 8.** Donor- acceptor interaction of a donating host with an acceptor- compound

we excluded unfavourable conformations and considered only those bonds marked in scheme 9.

60 degree increments were used for the torsion and 91 different conformers were received. After MM2-minimization all structures were optimized by PM3. The plot of the distribution of all 91 starting structures after the minimization shown in figure 7 resembles the conformational flexibility of compound **19**. Due to the flexibility of the host molecule the energy differences between the conformers, which are shown at the x-axis of figures 7 and 8, are small with some exceptions (cf. figure 7). There are only a few high energy conformations with high strain energy contributions during the MM2-preoptimization, whereas the size of the cavity differs a lot.

Figure 8 shows the result of the semiempirical optimization and proves that the different flexibility leads to a distribution of all structures over a range of 20 kcal/mol.

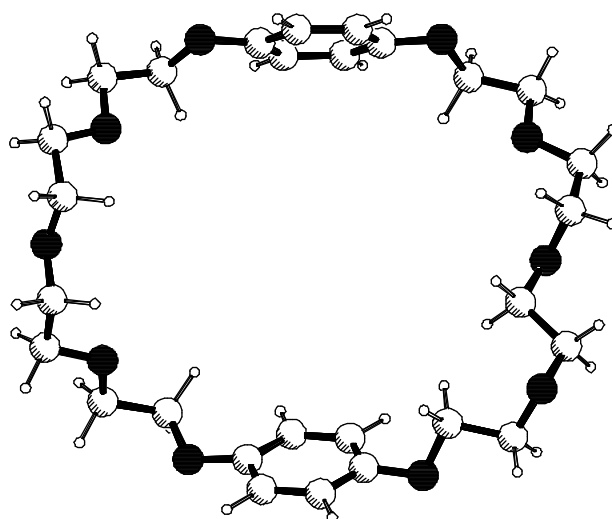
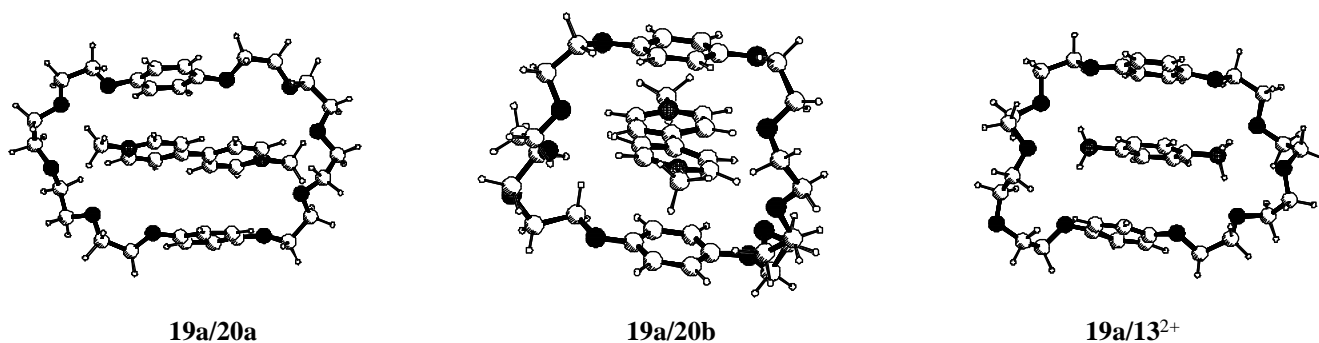


Table 10. ΔH_f of guests 20^{2+} and 13^{2+} , of the molecular complexes and the interaction energy with host **19**

PM3	Host 19				
Guest	Energy of guest ΔH_f (kcal/mol)		Energy of complex 19 + guest ΔH_f (kcal/mol)	Interaction energy (kcal/mol)	Link
20a	425.8	face-to-face	60.3	-31.3	45
20b	425.8	square	65.7	-25.9	46
13^{2+}	402.1	face-to-face	12.2	-55.8	47

**Figure 10.** Host **19a** with intercalated guests **20a**, **20b** and 13^{2+} .

Compound **19a** is according to the PM3 calculation almost 20 kcal/mol more stable than **19b**, but the phenyl rings are very close together and in a very unfavourable conformation for the inclusion of compounds (cf. figure 9). It is known [22], that a unreasonable stabilization is calculated for this geometrical arrangement, where the interaction between two phenyl rings is overestimated [23]. Compound **19b** is very similar to the published X-ray structure [21] and its values

for r_7 to r_9 are more favourable for the inclusion of guests. For the definition of r_7 to r_9 see scheme 9 and table 9. So **19b** was chosen as the starting geometry of the host molecule.

According to scheme 8 useful guest molecules should carry a positive charge. Therefore we have chosen two dications as guests: paraquatdication (20^{2+}) and diprotonated p-phenyldiamine (13^{2+}). There are experimental data available for 20^{2+} . From an association constant K_a of $730 \text{ dm}^3 \cdot \text{mol}^{-1}$ a free enthalpy G^0 of -3.9 kcal/mol was calculated for the complex with **19** [24]. Furthermore it is known from the X-ray structure that the molecular structure of **19** does not change in the molecular complex with 20^{2+} . PM3 calculates two different minima for the complex of **19** with 20^{2+} (table 10). One is almost identical with the X-ray structure [24], where the paraquatdication is incorporated in the crown. All

Table 11. Calculated Catenanes

PM3		ΔH_f (kcal/mol)	Interaction energy (kcal/mol)	Link
21a	$1^{4+} + 19$ stacked	700.86	-35.88	48
21b	$1^{4+} + 19$	700.03	-36.73	49
22	9 + 19	699.76	-44.27	50
23	11 + 19	703.75	-38.47	51

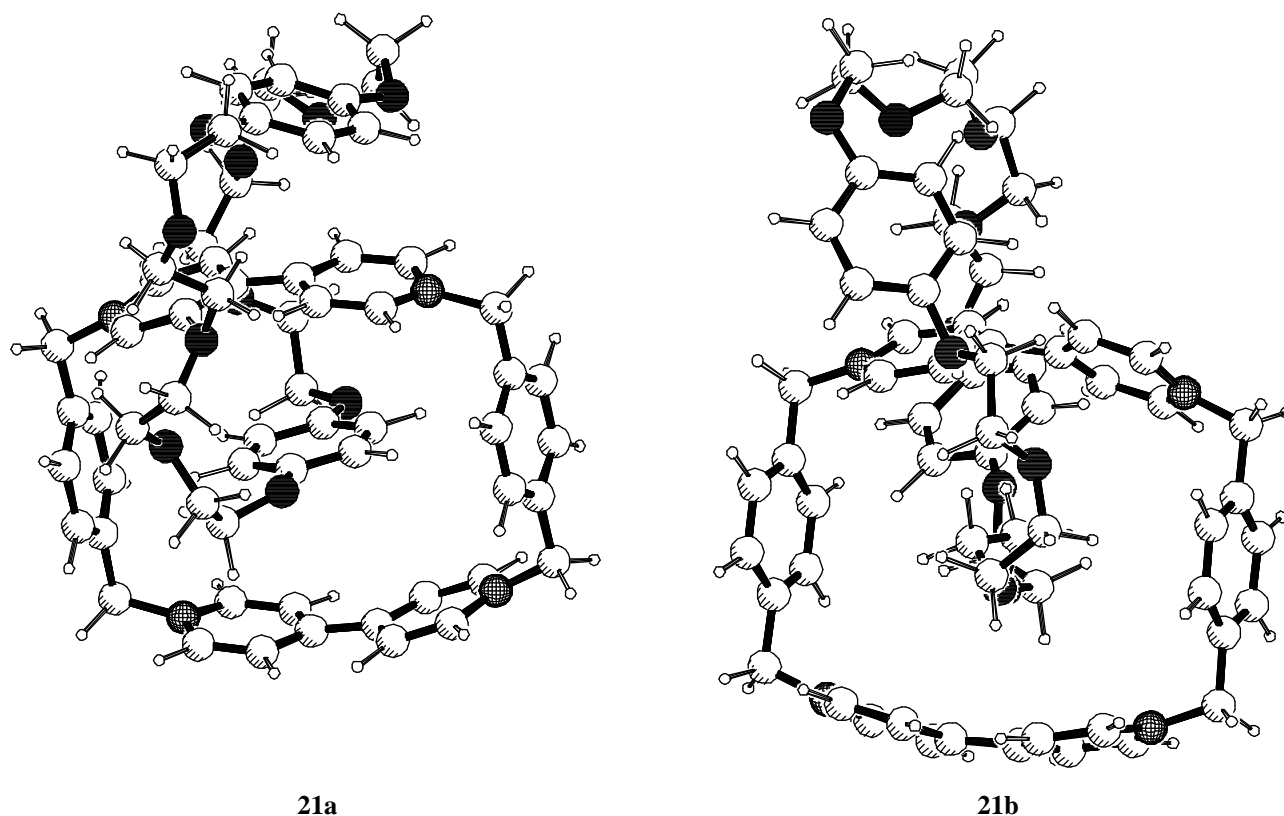


Figure 11. PM3 calculated structures of compounds **21a** and **21b**.

oxygens are pointing towards the nitrogen atoms, the phenyl rings are stacked in a distance of 4 Å and the conformation of the crown looks like a chair conformation. The other minimum is a structure where 20^{2+} is square to the orientation of the crown. All oxygens are pointing towards one nitrogen, the distance between the phenyl rings is further (5.5 and 4.8 Å) and the crown adopts a boat conformation (cf. figure 10). The partial charges reflect the difference between both structures. All 'coordinated' nitrogen atoms show the same partial charges, while the nitrogen which is pointing out of compound **20b** is 0.03 less positive than all other nitrogen atoms. Another destabilizing influence is the torsion of 15 degree within the bipyridine unit in **20b**. This leads to a decrease in the overlap and this results in a 5.4 kcal/mol higher heat of formation.

The interaction of the dication 13^{2+} with **19** gives the most stable complexes of this study. The interaction energy is calculated for compound **19b**. This is reasonable cause the interaction of the phenyl rings in a distance of 3.6 Å is very favourable and additionally there is a strong donor-acceptor interaction between the nitrogen atoms and the donating oxygens.

Catenane

The calculated catenanes were built from an electron donating and an electron accepting macrocycle. Catenane **21** was built from cyclobis(paraquat-p-phenylene) (1^{4+}) and the crown ether **19**. All catenanes are optimized without the keyword PRECISE, their gradient norms are between 0.3 – 0.4. From our previous results we could expect a catenane where the phenyl rings are stacked as in **20a**, but is the conformation of **20b** also stabilized in a catenane? The results are shown in table 11. Compound **21a** is very similar to **20a**, all oxygens are again pointing toward nitrogen atoms and the phenyl rings are stacked in a distance of 4 Å. This results in a comparably high interaction energy of about 36 kcal/mol. Probably this is only a local minimum, but the catenanes **21** have so many degrees of freedom, that a detailed analysis of the conformational hypersurface would make hundreds of calculations necessary. On the other hand, it would not provide so much more information for our study. Comparing the energy difference between **20a** and **20b** with the difference between **21a** and **21b** it is even more obvious that **21a** is probably not the global minimum which should be even lower in energy. Figure 11 shows the calculated geometries of **21a** and **21b**. Experimental data of two other catenanes, **22** and **23**, built from compounds **9** and **11** with the same crown ether **19** are available [25]. Their geometrical arrangement is very similar to **21a**. The phenyl rings of the crown ether are stacked in

distances of 3.6 to 3.8 Å within the macrocycle and about 4.2 Å outside due to the larger flexibility of the crown ether chain. The phenylene ring outside is not exactly above the other three rings. It is slightly twisted against their planes. Their interaction energy is also very high, so they should be easy to synthesize.

Conclusion

The concept of self-organization was examined using the semiempirical PM3 Hamiltonian. The experimentally known inclusion complexes could be reproduced and the results compare well with known experimental data and X-ray structures. π -stacking and electrostatics are the driving forces responsible for the formation of those molecular complexes. Cyclobis(paraquat-p-phenylene) (1^{4+}) is an exceptional compound and the only macrocycle from a series of compounds with similar geometry for which stable molecular complexes could be calculated. The calculated catenanes give high interaction energy values and due to our results it should be possible to create catenanes which are not known yet.

Acknowledgment. We gratefully acknowledge the helpful discussions with Prof. Dr. A. Mehlhorn and Prof. Dr. J. Fabian (TU Dresden) and their continuing interest in this study. One of us (C.R.) thanks for financial support by the *Deutsche Forschungsgemeinschaft* (Graduiertenkolleg: Struktur-Eigenschaftsbeziehungen bei Heterocyclen).

References

1. a) for a review see Philp, D.; Stoddart, J.F., *Angew. Chem.* **1996**, *108*, 1242. b) Lindsey, J.S. *New J. Chem.* **1991**, *15*, 153. c) Philp, D.; Stoddart, J.F. *Synlett* **1991**, 445. d) Whitesides, G.M.; Mathias, J.P.; Seto, C.T. *Science* **1991**, *254*, 1312.
2. Odell, B.; Reddington, M.V.; Slawin, A.M.Z.; Spencer, N.; Stoddart, J.F.; Williams, D.J. *Angew. Chem., Int. Ed. Engl.* **1988**, *27*, 1547.
3. a) Ashton, P.R.; Perez-Garcia, L.; Stoddart, J.F.; White, A.J.P.; Williams, D.J. *Angew. Chem.* **1995**, *107*, 607. b) Ashton, P.R.; Bisell, R.A.; Spencer, N.; Stoddart, J.F.; Tolley, M.S. *Synlett* **1992**, 914. c) Ashton, P.R.; Bisell, R.A.; Gorski, R.; Philp, D.; Spencer, N.; Stoddart, J.F.; Tolley, M.S. *ibid.* **1992**, 919. d) Cordova, E.; Bisell, R.A.; Spencer, N.; Ashton, P.R.; Stoddart, J.F.; Kaifer, A.E. *J. Org. Chem.* **1993**, *58*, 6550. e) Bisell, R.A.; Cordova, E.; Kaifer, A.E.; Stoddart, J.F. *Nature* **1994**, *369*, 133. f) Wenz, G. Keller, B. *Angew. Chem. Int. Ed. Engl.* **1992**, *31*, 197. g) Stoddart, J.F. *Angew. Chem. Int. Ed. Engl.* **1992**, *31*, 846. h) Amabilino, D.B.; Ashton, P.R.; Brown, C.L.; Cordova, E.; Godinez, L.A.; Goodnow, T.T.; Kaifer, A.E.; Newton, S.P.; Pietraszkiewicz, M.; Philp, D.; Raymo, F.M.; Reder, S.; Rutland, M.T.; Slawin, A.M.Z.; Spencer, N.; Stoddart, J.F.; Williams, D.J. *J. Am. Chem. Soc.* **1995**, *117*, 1271. i) Amabilino, D.B.; Ashton, P.R.; Stoddart, J.F.; Menzer, S.; Williams, D.J. *J. Chem. Soc., Chem. Commun.* **1994**, 2475. k) Amabilino, D.B.; Ashton, P.R.; Brown, C.L.; Hayes, W.; Stoddart, J.F.; Tolley, M.S.; Williams, D.J. *J. Chem. Soc., Chem. Commun.* **1994**, 2479. l) Ashton, P.R.; Blower, M.A.; Iqbal, S.; McLean, C.H.; Stoddart, J.F.; Tolley, M.S.; Williams, D.J. *Synlett*, **1994**, 1059. m) Ashton, P.R.; Blower, M.A.; McLean, C.H.; Stoddart, J.F.; Tolley, M.S. *Synlett*, **1994**, 1063.
4. Amabilino, D.B.; Ashton, P.R.; Reder, A.S.; Spencer, N.; Stoddart, J.F. *Angew. Chem.* **1994**, *106*, 1316.
5. a) Goodnow, T.T.; Reddington, M.V.; Stoddart, J.F.; Kaifer, A.E. *J. Am. Chem. Soc.* **1991**, *113*, 4335. b) Bernardo, A.R.; Stoddart, J.F.; Kaifer, A.E. *J. Am. Chem. Soc.* **1992**, *114*, 10624.
6. a) Ashton, P.R.; Odell, B.; Reddington, M.V.; Slawin, A.M.Z.; Stoddart, J.F.; Williams, D.J. *Angew. Chem.* **1988**, *100*, 1608. b) Reddington, M.V.; Slawin, A.M.Z.; Spencer, N.; Stoddart, J.F.; Vicent, C.; Williams, D.J. *J. Chem. Soc., Chem. Commun.* **1991**, 630.
7. Philip, D.; Slawin, A.M.Z.; Spencer, N.; Stoddart, J.F.; Williams, D.J. *J. Chem. Soc., Chem. Commun.* **1991**, 1584.
8. a) Vögtle, F.; Müller, W.M.; Müller, U.; Bauer, M. Rissanen, K. *Angew. Chem.* **1993**, *105*, 1356. b) Hunter, C.A. *J. Am. Chem. Soc.* **1992**, *114*, 5303. c) Vögtle, F.; Meier, S.; Hoss, R. *Angew. Chem.* **1992**, *104*, 1628; *Angew. Chem. Int. Ed. Engl.* **1992**, *31*, 1619. d) Gunter, M.J.; Johnston, M.R. *J. Chem. Soc., Chem. Commun.* **1994**, 829. e) Gunter, M.J.; Hockless, M.R.; Johnston, M.R.; Skelton, B.W.; White, A.H. *J. Am. Chem. Soc.* **1994**, *116*, 4810. f) Benniston, A.C.; Harriman, A. *Angew. Chem.* **1993**, *105*, 1553, *Angew. Chem. Int. Ed. Engl.* **1993**, *32*, 1459. g) Benniston, A.C.; Harriman, A.; Lynch, V.M. *Tetrahedron Lett.*, **1994**, *35*, 1473.
9. a) Hunter, C.A.; Sanders, J.M. *J. Am. Chem. Soc.*, **1990**, *112*, 5525. b) Kobayashi, K.; Asakawa, Y.; Kikuchi, Y.; Toi, H.; Aoyama, Y. *J. Am. Chem. Soc.*, **1993**, *115*, 2648.
10. a) for recent reviews of hydrogen bonding in molecular recognition, see: Diederich, F.N. in 'Cyclophanes'; Royal Society of Chemistry: London, 1991. Hamilton, A.D. 'Advances in Supramolecular Chemistry': Gokel, G., Ed.; Jai Press, Greenwich, CT, 1990, Vol. 1, p.1. b) Rodriguez, J. *J. Comp. Chem.* **1994**, *15*, 183. c) Zheng, Y.; Merz, Jr., M. *J. Comp. Chem.* **1992**, *13*, 1151. d) Hunter, C.A.; Sanders, J.K.M. *J. Am. Chem. Soc.*, **1990**, *112*, 5525. e) Edwards, W.E.; Du, M.; Royal, J.S.; McHale, J.L. *J. Phys. Chem.* **1990**, *94*, 5748. f) Glauser, W.A.; Raber, D.J.; Stevens, B. *J. Phys. Chem.* **1989**, *93*, 1784. g) Glauser, W.A.; Raber, D.J.; Stevens, B. *J. Comp. Chem.* **1988**, *9*, 539. h) Cioslowski, J.; Turek, A.M. *Z. Naturforsch.* **1985**, *40a*, 1299. i) Mo, O.; Yanez, M.; Fernandez-Alonso, J.I. *J. Phys. Chem.* **1975**, *79*, 137.

11. a) Stewart, J.J.P. *J. Comp. Chem.* **1989**, *10*, 209. b) Stewart, J.J.P. *J. Comp. Chem.* **1989**, *10*, 221.
12. a) Rauhut, G.; Alex, A.; Chandrasekhar, J.; Steinke, T.; Sauer, W.; Beck, B.; Clark, T., VAMP 5.5, Oxford Molecular Group, The Magdalen Centre, Oxford Science Park, Sandford-on-Thames, Oxford OX4 4GA, UK, **1994**.
13. Baker, J. *J.Comp.Chem.* **1986**, *7*, 385.
14. PCModel 3.0, Serena Software, Bloomington, **1988**.
15. a) Allinger, N.L. *J. Am. Chem. Soc.*, **1977**, *99*, 8127. b) Burkert, U.; Allinger, N.L. *J. Comp. Chem.* **1982**, *3*, 40
16. Spartan 4.0, Wavefunction, Inc., Van Karman #370, Irvine, CA 92715, USA.
17. Geuder, W.; Hünig, S.; Suchy, A. *Angew. Chem.* **1983**, *95*, 501.
18. Ashton, P.R.; Goodnow, T.T.; Kaifer, A.E.; Reddington, M.V.; Slawin, A.M.Z.; Spencer, N.; Stoddart, J.F.; Vicent, C.; Williams, D.J. *Angew. Chem., Int. Ed. Engl.* **1989**, *28*, 1396.
19. Domscke, G.; Scheytza, H. private communication.
20. Exner, O. Critical Compilation of Substituent Constants in Correlation Analysis in Chemistry, 439, Plenum Press, Chapman, N.B.; Shorter, J.; Edts., New York & London, 1978,
21. Allwood, B.L.; Spencer, N.; Shahriari-Zavarek, H.; Stoddart, J.F.;Williams, D.J. *J. Chem. Soc., Chem. Commun.* **1987**, 1061.
22. a) Petterson, I.; Liljefors, T. *J. Comp. Chem.* **1987**, *8*, 1139. b) Allinger, N.L.; Lii, J.H. *J. Comp. Chem.* **1987**, *8*, 1146. c) Ivanow, P.M.; Momchilova, T.G. *J. Mol. Struct. (Theochem)*, **1991**, *233*, 115.
23. a) Kim, D.H.; Lee, S.S.; Whang, D.; Kim, K. *Bioorg. & Med. Chem. Lett.*, 1993, *3*, 263. b) Muehldorf, A.V.; Engen, D.V.; Warner, J.C., Hamilton, A.D. *J. Am. Chem. Soc.*, **1988**, *110*, 6561. c) Ortholand, J.Y.; Slawin, A.M.Z.; Spencer, N.; Stoddart, J.F.;Williams, D.J. *Angew. Chem.*, **1989**, *101*, 1402.
24. Allwood, B.L.; Spencer, N.; Shahriari-Zavarek, H.; Stoddart, J.F.;Williams, D.J. *J. Chem. Soc., Chem. Commun.* **1987**, 1064.
25. Amabilino, D.B.; Ashton, P.R.; Tolley M.S.; Stoddart, J.F.;Williams, D.J. *Angew. Chem.*, **1993**, *105*, 1358.